Rotational Spectrum, Electric Dipole Moment, Quadrupole Coupling, and Partial r_0-Structure of 3-Cyanothiophene

J. Wiese and D. H. Sutter

Abteilung Chemische Physik im Institut für Physikalische Chemie
der Christian Albrechts Universität, Kiel

(Z. Naturforsch. **32 a**, 890—896 [1977]; received July 7, 1977)

The microwave rotational spectrum of the most abundant species of 3-Cyanothiophene was investigated for the ground vibrational state. Rotational constants and centrifugal distortion constants are given. The electric dipole moment components μ_a and μ_b and the ^{14}N-quadrupole coupling constant $\chi_+ = \chi_{bb} + \chi_{cc}$ were determined from the Stark-effect splittings and hfs-splittings respectively. The experimental results are compared to CNDO/2 calculations and are discussed with reference to ring distortion.

In the following we present the results of a study of the microwave rotational spectrum of 3-Cyanothiophene. Together with the data obtained for 2-Cyanothiophene [1] and 2-Cyanofurane [2] they may provide a basis for a subsequent analysis of the rotational Zeeman effect [3] in these CN-substituted aromatic rings.

Experimental

The sample was prepared by a reaction of 3-Bromothiophene with Copper(I) cyanide in Quinoline [4]:

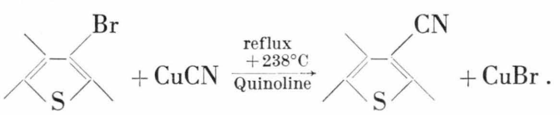

After a vacuumdestillation 3-Cyanothiophene was separated from rests of Quinoline and 3-Bromothiophene by gaschromatography. A conventional Stark-effect modulated microwave spectrometer described previously [5, 6] was used to record the spectrum in the X-through Q-band region. The spectrometer is equipped with phase stabilized backward wave oszillators as monochromatic [7] radiation sources together with an oversized X-band wave guide absorption cell with an inner cross section of 1 by 5 cm to provide a sufficiently uniform Stark-field over the absorption volume [8, 9]. Typical recording conditions were: sample pressures in the range from 1 to 20 mTorr and sample temperatures in the range from -20 to $+10$ °C. 33 kHz Stark-effect square wave modulation was used throughout.

Reprint requests to Prof. Dr. D. H. Sutter, Abt. Chemische Physik im Institut für Physikalische Chemie, Universität Kiel, Olshausenstraße 40/60, *D-2300 Kiel*.

Under these conditions typical recorded linewidths were on the order of 300 to 400 kHz full halfwidth at half height. Figure 1 shows an example.

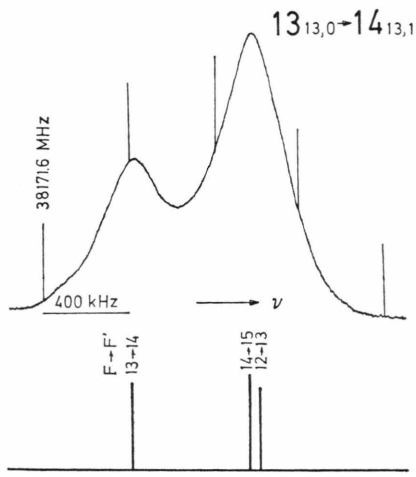

Fig. 1. Partly resolved ^{14}N hyperfine structure of the $13_{13,0} \to 14_{13,1}$ and $13_{13,1} \to 14_{13,2}$ rotational transitions of 3-Cyanothiophene in its vibrational ground state. The frequencies and hyperfine patterns of the two transitions coincide within better than 1 kHz. The bar pattern at the bottom was calculated using $\chi_+ = 4.12$ MHz from Table 4.

Rotational Constants

The rotational spectrum of 3-Cyanothiophene exhibits fairly strong μ_a-type transitions while the μ_b-type transitions are very low in intensity and could not be observed all. Table 1 gives a list of recorded transitions. Transitions with intermediate K_--values were not included in this listing since for these transitions ^{14}N quadrupole coupling causes very narrow multiplet splittings leading to broadened

Rotational transition $J_{K_-K_+}$	$\rightarrow J'_{K'_-K'_+}$	ν_{exp} [MHz]	ν_{rr} [MHz]	ν_{cd} [MHz]	$\nu_{\text{exp}}-\nu_{cd}$ [kHz]
$3_{0\,3}$	$4_{0\,4}$ *	10808.667	10808.654	10808.668	−1
$3_{1\,2}$	$4_{1\,3}$ *	11394.832	11394.810	11394.827	5
$3_{1\,3}$	$4_{1\,4}$ *	10360.955	10360.889	10360.888	67
$3_{2\,1}$	$4_{3\,2}$ *	39639.960	39639.972	39640.092	−132
$3_{2\,2}$	$4_{3\,1}$ *	39684.917	39684.819	39684.939	−22
$4_{0\,4}$	$5_{0\,5}$ *	13447.532	13447.565	13447.575	−43
$4_{1\,3}$	$5_{1\,4}$ *	14225.926	14225.888	14225.900	26
$4_{1\,4}$	$5_{1\,5}$ *	12935.946	12935.963	12935.956	−10
$5_{1\,4}$	$6_{1\,5}$ *	17044.135	17044.180	17044.183	−48
$5_{1\,5}$	$6_{1\,6}$ *	15501.884	15501.897	15501.880	4
$6_{2\,5}$	$6_{3\,4}$ *	28924.770	28924.709	28924.726	44
$6_{0\,6}$	$7_{0\,7}$	18607.678	18607.704	18607.688	−10
$6_{0\,6}$	$7_{1\,7}$	21567.419	21567.425	21567.391	28
$6_{1\,5}$	$7_{1\,6}$	19846.074	19846.094	19846.080	−6
$6_{2\,4}$	$7_{2\,5}$	19457.790	19457.775	19457.716	74
$6_{2\,5}$	$7_{2\,6}$	18999.006	18999.068	18999.007	−1
$6_{5\,1}$	$7_{5\,2}$	19097.433	19097.779	19097.400	33
$6_{6\,0}$	$7_{6\,1}$	19090.700	19091.239	19090.695	5
$7_{0\,7}$	$8_{0\,8}$	21128.545	21128.518	21128.541	4
$7_{0\,7}$	$8_{1\,8}$	23562.613	23562.777	23562.710	−97
$7_{1\,6}$	$8_{1\,7}$	22627.461	22627.505	22627.467	−6
$7_{1\,7}$	$8_{1\,8}$	20603.020	20603.055	20603.007	13
$7_{2\,5}$	$8_{2\,6}$	22345.263	22345.376	22345.290	−27
$7_{2\,6}$	$8_{2\,7}$	21684.306	21684.386	21684.301	5
$7_{6\,1}$	$8_{6\,2}$	21822.904	21823.549	21822.910	−6
$7_{7\,0}$	$8_{7\,1}$	21816.941	21817.783	21826.921	20
$8_{1\,8}$	$8_{2\,7}$	22057.226	22057.099	22057.140	86
$8_{7\,1}$	$9_{7\,2}$	24548.659	24549.645	24548.653	6
$8_{2\,7}$	$8_{3\,6}$	29242.617	29242.752	29242.606	11
$8_{0\,8}$	$9_{1\,9}$	25571.786	25571.877	25571.774	12
$8_{1\,8}$	$9_{0\,9}$	21182.199	21182.216	21182.184	15
$8_{8\,0}$	$9_{8\,1}$	24543.122	24544.382	24543.101	21
$9_{0\,9}$	$10_{0\,10}$	26079.562	26079.676	26079.579	−17
$9_{1\,8}$	$10_{2\,9}$	38820.194	38820.417	38820.142	52
$9_{9\,0}$	$10_{9\,1}$	27269.214	27271.016	27269.201	13
$10_{1\,10}$	$10_{1\,9}$	13925.416	13925.195	13925.305	111
$10_{3\,7}$	$10_{4\,6}$	39835.700	39854.321	39835.675	25
$12_{1\,11}$	$13_{1\,12}$	36056.942	36057.232	36056.940	2
$12_{3\,9}$	$13_{3\,10}$	36080.816	36081.303	36080.811	5
$12_{11\,1}$	$13_{11\,2}$	35451.698	35455.317	35451.313	−15
$12_{12\,0}$	$13_{12\,1}$	35446.781	35451.031	35446.787	−6
$13_{13\,0}$	$14_{13\,1}$	38172.338	38177.725	38172.350	−12
$15_{1\,15}$	$15_{1\,14}$	28124.106	28124.514	28124.327	−221
$17_{1\,17}$	$17_{1\,16}$	34056.248	34056.593	34056.134	114
$20_{2\,19}$	$20_{2\,18}$	28702.487	28703.805	28702.477	10

Table 1. Rotational transition frequencies, ν_{exp} of the most abundant species of 3-Cyanothiophene in its ground vibrational state. Listed frequencies are intensity weighted center frequencies of the hyperfine multiplets [13]. The transitions marked by an asterisk were used for the least squares fit of the rigid rotor rotational constants given in Table 2. ν_{rr} and ν_{cd} denote the frequencies calculated from the rigid rotor rotational constants and from the rotational constants and centrifugal distortion constants listed in Table 3 respectively.

lines which could not be resolved into individual components. The rigid rotor rotational constants, which were fitted to the observed transition frequencies as described in Ref. 2, are listed in Table 2. By the small value of the inertia defect it is confirmed that the equilibrium configuration of the molecules is planar.

As is seen from Table 1 the rigid rotor model applies to fairly high values of J, provided K_- ($=K_a$) is small. For K_--values close to J centrifugal distortion becomes appreciable at lower J-values. Therefore the complete set of recorded transitions was also subjected to a centrifugal distortion analysis according to Watson [10]. The corresponding effective rotational Hamiltonian is given in Eq. (1)[11].

$$\begin{aligned}\hat{\mathcal{H}}_{\text{eff}}/h = {} & A\,\hat{J}_a^2 + B\,\hat{J}_b^2 + C\,\hat{J}_c^2 \\ & - \Delta_J\,\hat{J}^4 - \Delta_{JK}\,\hat{J}^2\,\hat{J}_a^2 - \Delta_K\,\hat{J}_a^4 \\ & - \delta_J\,[\hat{J}^2(\hat{J}_b^2-\hat{J}_c^2) + (\hat{J}_b^2-\hat{J}_c^2)\hat{J}^2] \\ & - \delta_K\,[\hat{J}_a^2(\hat{J}_b^2-\hat{J}_c^2) + (\hat{J}_b^2-\hat{J}_c^2)\hat{J}_a^2]; \quad (1)\end{aligned}$$

$A, B, C =$ rotational constants.

$\hat{J}^2 = \hat{J}_a^2 + \hat{J}_b^2 + \hat{J}_c^2$ = square of the overall angular momentum operator (measured in units of $\hbar$).

$\hat{J}_a, \hat{J}_b, \hat{J}_c$ = operators corresponding to the components of the angular momentum in direction of the principal inertia axes (measured in units of $\hbar$).

$\Delta_J, \Delta_{JK}, \Delta_K, \delta_J, \delta_K$ = centrifugal distortion constants.

Table 2. Rigid rotor rotational constants fitted to those transitions in Table 1 which are marked by an asterisk. The given uncertainties are single standard deviations of the least squares fit. For the conversion from rotational constants to moments of inertia 505.531 GHz amu Å^2 was used as conversion factor [21]. The small value of the inertia defect is typical for molecules with a planar equilibrium configuration.

$A_0 = 7.115\,103(6)$ GHz	$I_{aa} = 71.050\,4(4)$ amu Å^2
$B_0 = 1.491\,292(2)$ GHz	$I_{bb} = 338.988\,6(4)$ amu Å^2
$C_0 = 1.232\,536\,(1)$ GHz	$I_{cc} = 410.155\,2(3)$ amu Å^2
$\Delta I = I_{aa}+I_{bb}-I_{cc} = 0.116(1)$ amu Å^2	

The results of the least squares fit including centrifugal distortion are given in Table 3. Also given in this Table are the corresponding τ-values. Even so no restriction was imposed on the centrifugal distortion constants during the least squares procedure the planarity condition [12].

$$\tau_2 \overset{!}{=} C\tau_1 + (A+B)\tau_{cccc}$$

turns out to be well fullfilled by the resultant τ-values. The rotational constants will be discussed below with reference to the distortion of the ring due to $-C{\equiv}N$ substitution.

^{14}N Quadrupole Coupling Constants

The quadrupole hyperfine structure [18] of the μ_a-type transitions shows much similarity to the one expected for a prolate symmetric top i.e. $J \rightarrow J+1$ transitions involving $K_- = J-1$ and $K_- = J$ are split most. With $A > B \sim C$ (Table 2) and the C≡N bond closely parallel to the a-axis of the moment of inertia tensor (see Fig. 2) this is not surprising.

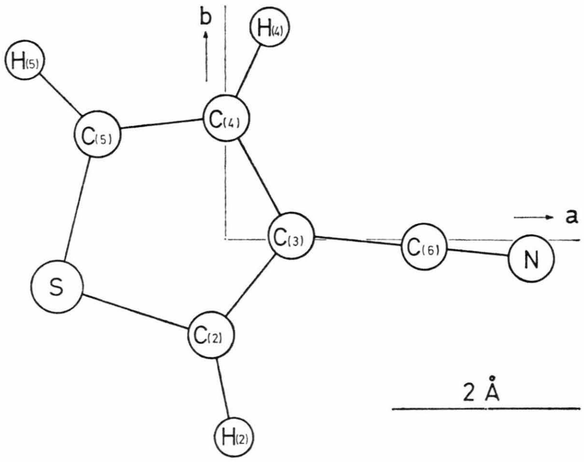

Fig. 2. Labeling of atoms and orientation of the principal inertia axes system in 3 Cyanothiophene. During the fit to the observed rotational constants only the bond angle $\sphericalangle C_{(2)}C_{(3)}C_{(6)}$ and the bond distance $^rC_{(2)}C_{(3)}$ (with corresponding slight changes of $\sphericalangle C_{(2)}C_{(3)}C_{(4)}$ and $\sphericalangle C_{(3)}C_{(4)}C_{(5)}$) were adjusted to the experimental values for A, B and C.

Table 4 gives a list of partly resolved hyperfine multiplets. These splittings were used to fit the sum of the b- and c-quadrupole coupling constants by a least squares procedure. $\chi_- = \chi_{bb} - \chi_{cc}$ was set to zero during the fit. Within the experimental uncertainties this procedure is reasonable since these splittings are almost independent on χ_- (a χ_--value even as big as 4 MHz would cause only minor changes well below 10 kHz. For comparison: $\chi_- = 0.96$ MHz in the related molecule 2-Cyanofurane).

Table 3. Rotational constants and centrifugal distortion constants resulting from a least squares fit to the complete set of rotational transition frequencies listed in Table 1. Also given are the correlation matrix and the corresponding τ-values. The planarity condition $\tau_2 \overset{!}{=} C\tau_1 + (A+B)\tau_{cccc}$ was not used during the fit. However it turns out to be well fullfilled by the resulting τ-values.

A	7.115180 GHz	±13 kHz	1.0								
B	1.491299 GHz	± 2 kHz	−0.07	1.0							
C	1.232535 GHz	± 2 kHz	−0.04	0.71	1.0						
Δ_J	0.043 kHz	± 0.007 kHz	0.00	0.70	0.81	1.0					
Δ_{JK}	1.028 kHz	± 0.015 kHz	0.03	−0.14	−0.35	−0.66	1.0				
Δ_K	1.97 kHz	± 0.72 kHz	0.92	−0.11	−0.07	0.00	−0.03	1.0			
δ_J	0.0089 kHz	± 0.0009 kHz	0.00	0.43	−0.28	−0.09	0.30	−0.04	1.0		
δ_K	0.670 kHz	± 0.076 kHz	−0.23	−0.18	−0.10	0.08	−0.31	−0.18	−0.58	1.0	

$\tau_{aaaa} = -12.178$ kHz $\tau_{bbbb} = -0.234$ kHz $\tau_{cccc} = -0.101$ kHz

$\tau_1 = -4{,}630$ kHz $\tau_2 = -6{,}594$ kHz

Table 4. Quadrupole hyperfine doublets of some high-K_- μ_a-type transitions used for the least squares fit of $\chi_+ = \chi_{bb} + \chi_{cc}$. As indicated each doublet consists of a superposition of two rotational transitions which whithin 1 kHz have the same center frequencies and hyperfine splittings. Furthermore the more intense component of each doublet consists of two unresolved hyperfine satellites. Listed frequencies give the peak frequency of this component which was taken as the intensity weighted mean of its two (4) constituents. The last two columns were calculated using the least squares value for $\chi_+ = 4.12 \pm 0.06$ MHz. χ_- was set to zero.

Rotational transition $J_{K_-K_+} \rightarrow J'_{K'_-K'_+}$	$F \rightarrow F'$	rel. int. %	ν_{exp} [MHz]	$\nu_{split. exp}$ [MHz]	$\Delta\nu_{calc}$ [MHz]		$\nu_{split. calc}$
$6_{51}-7_{52}$	$7-8$	37.8	19097.648		0.180	0.231	
and	$5-6$	28.2			0.300		
				0.648			0.691
$6_{52}-7_{53}$	$6-7$	32.7	19097.000		−0.460		
$6_{60}-7_{61}$	$7-8$	37.8	19091.040		0.254	0.334	
and	$5-6$	28.2			0.442		
				1.021			0.996
$6_{61}-7_{62}$	$6-7$	32.7	19090.014		−0.662		
$7_{61}-8_{62}$	$8-9$	37.3	21823.121		0.177	0.222	
and	$6-7$	28.9			0.280		
				0.655			0.664
$7_{62}-8_{63}$	$7-8$	32.8	21822.466		−0.442		
$7_{70}-8_{71}$	$8-9$	37.3	21817.239		0.238	0.303	
and	$6-7$	28.9			0.386		
				0.900			0.904
$7_{71}-8_{72}$	$7-8$	32.8	21816.339		−0.601		
$8_{71}-9_{72}$	$9-10$	36.8	24548.870		0.172	0.212	
and	$7-8$	29.4			0.261		
				0.637			0.633
$8_{72}-9_{73}$	$8-9$	32.9	24548.233		−0.421		
$8_{80}-9_{81}$	$9-10$	36.8	24543.399		0.223	0.276	
and	$7-8$	29.4			0.343		
				0.835			0.825
$8_{81}-9_{82}$	$8-9$	32.9	24542.564		−0.549		

Since the experimental information on χ_- is essentially contained in low intensity satellites of some low-J μ_a-type transitions as well as in several μ_b-type transitions all of them with intensities below the sensitivity of the spectrograph, no experimental χ_--value can be given at the present stage.

Electric Dipole Moment

The absolute values for the components of the electric dipole moment were determined from the Stark effect observed for the $4_{23} \rightarrow 5_{24}$, $4_{04} \rightarrow 5_{05}$ and $4_{14} \rightarrow 5_{15}$ rotational transitions (Table 5). All these transitions show neglegible ^{14}N quadrupole hyperfinestructure which simplifies the analysis. The Stark field was calibrated using OCS, $J=0 \rightarrow J'=1$ as standard [19].

For the analysis of the Stark effect the nuclear quadrupole coupling was neglected and the splittings were calculated within the frame of second order perturbation theory [14]. Within this approximation the shifts of the Stark-effect sublevels with respect to the zero field sublevels are given by Eq. (2):

$$W_{J\tau M}(E) - W_{J\tau M}(0) = E^2 \left([A'_{aJ\tau} + M^2 B'_{aJ\tau}]\, \mu_a^2 + [A'_{bJ\tau} + M^2 B'_{bJ\tau}]\, \mu_b^2 \right) \tag{2}$$

$W_{J\tau M}(E)$ = energy of the rotational sublevel designated by the rotational quantum numbers $J\tau M$ in the presence of a Stark field E;

μ_a, μ_b = vibronic ground state expectation values for the components of the molecular electric dipole moment in direction of the principal inertia axes ($\mu_c = 0$ due to the planarity of the molecule)

$A'_{aJ\tau}$, $A'_{bJ\tau}$, $B'_{aJ\tau}$, $B'_{bJ\tau}$ = coefficients which arise from perturbation sums over direction cosine matrix elements. They may be calculated once the rotational constants are known (see Ref. [14]).

According to Eq. (2) the splittings listed in Table 5 lead to a set of equations which are linear in μ_a^2 and μ_b^2 from which the latter were calculated by a least squares fit. Due to the fact that the $M=0$

Rotational transition and zero field frequency	Projection quantum number M_J	Stark field E (V/cm)	$\Delta\nu_{M\,exp}$ (MHz)	$\Delta\nu^{(2)}_{calc}$ (MHz)	$\Delta\nu^{(n)}_{calc}$ (MHz)
$4_{04}-5_{05}$	1	418.1	−0.918	−0.946	−0.944
13447.532	1	523.5	−1.482	−1.483	−1.478
	1	629.0	−2.110	−2.141	−2.133
$4_{14}-5_{15}$	1	629.0	−0.297	−0.372	−0.351
12935.946	1	840.3	−0.616	−0.663	−0.602
	1	1262.7	−1.403	−1.497	−1.209
	2	523.5	3.427	3.406	3.438
	2	629.0	4.918	4.918	4.961
	2	734.5	6.783	6.706	6.759
	3	418.1	6.202	6.072	6.105
	3	523.5	9.587	9.516	9.559
	3	629.0	13.612	13.740	13.765
$4_{23}-5_{24}$	0	629.0	−1.440	−1.489	−1.487
13599.680	0	734.5	−2.024	−2.030	−2.027
	0	840.3	−2.640	−2.657	−2.649
	0	945.8	−3.398	−3.366	−3.352
	0	1051.4	−4.162	−4.159	−4.143

Table 5. Stark-effect shifts $\Delta\nu_M = \nu_M(E) - \nu_M(0)$ which were used for the least squares fit of the a- and b-components of the molecular electric dipole moment. The selected transitions show neglegible ^{14}N-quadrupole hyperfine contributions. The column headed by $\Delta\nu^{(2)}_{calc}$ gives the shifts if calculated by second order perturbation theory from the optimized dipole moments listed in Table 6. For comparison shifts calculated by numerical diagonalization of the Hamiltonian are given in the column headed by $\Delta\nu^{(n)}_{calc}$. The calibration uncertainty of the electric field strength is 0.2%.

satellite of the $4_{23} \rightarrow 5_{24}$ transition depends mainly on the μ_b-component, the resultant normal equations are well conditioned and lead to the absolute values $|\mu_a| = 4.09 \pm 0.01$ and $|\mu_b| = 0.56 \pm 0.01$ D. The quoted errors are single standard deviations of the fit and do include the calibration uncertainty of the Stark field which was below 0.2%.

In order to check the validity of the second order approach, the resultant μ-values were used to recalculate the splittings by numerically diagonalizing the Hamiltonian matrix. In this procedure for each rational state only a finite submatrix including the neighbouring J values was set up in the limiting symmetric top basis and diagonalized by a Jacobi routine. The results are listed in the last column of Table 5. They confirm that the second order approximation is sufficient to describe the Stark-shifts of the satellites selected for the dipole moment determination. In Table 6 the experimental dipole moments are compared with the results of a CNDO-calculation and the values obtained by adding the dipole moments of Thiophene [($\mu = 4.14(5)$ Debye)[15]] and Benzonitrile [($\mu = 0.55(1)$ Debye[16])] vectorially.

Discussion

The experimental rotational constants may be used to get some preliminary information on the distortion of the ring upon CN-substitution. Chemical intuition suggests, that conjugation of the π-orbitals in the CN tripple bond and the adjacent double bond in the ring should lead to more double bond character in the latter. Thus as compared to Thiophene one would expect a shortening of the $r_{C(2)C(3)}$ distance (see Fig. 2) and a change of the bond angle $\sphericalangle C_{(2)}C_{(3)}C_{(6)}$ towards 120°. We therefore kept all other structural parameters fixed to their values in Thiophene and Benzonitrile respectively and adjusted $r_{C(2)C(3)}$ and $\sphericalangle C_{(2)}C_{(3)}C_{(6)}$ so as to optimally reproduce the observed rotational constants. This lead to the striking result (see Table 7) that the improved structure with $r_{C(2)C(3)}$ reduced to 1.346 Å ($r = 1.334$ Å for a "pure double bond"[20])

Table 6. Molecular electric dipole moment of 3-Cyanothiophene. The experimental values were determined by a least squares fit to the observed Stark-effect splittings (Table 5) using second order perturbation theory. The experimental uncertainties include a 0.2% calibration uncertainty of the Stark field. Only the absolute values of the components are obtained from the experiment. Also given for comparison are dipole moments calculated by the semiempirical CNDO/2 method (the upper indices refer to the structures given in Table 7), and by vectoraddition of the experimental dipole moments of Benzonitrile [16] (CN at negative end) and Thiophene [15] (index α: S at negative end; index β: S at positive end).

	$\|\mu_{exp}\|$ (Debye)	I CNDO/2 (Debye)	II CNDO/2 (Debye)	$\mu_{add}^{(\alpha)}$ (Debye)	$\mu_{add}^{(\beta)}$ (Debye)
μ_a	4.09(2)	−2.01	−1.92	−3.64	−4.60
μ_b	0.56(1)	+0.85	+0.90	+0.64	+0.11
$\|\mu_{total}\|$	4.13(2)	2.18	2.12	3.70	4.60

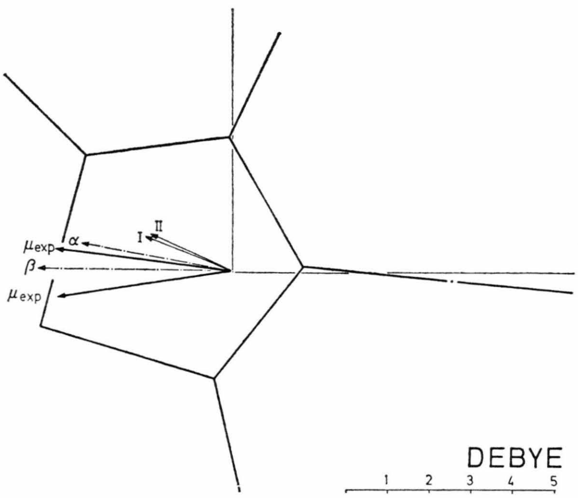

Fig. 3. Experimental and calculated dipole moments for 3-Cyanothiophene. Assuming the CN-group to be at the negative end of the molecule two orientations $\mu^{(1)}_{exp.}$ and $\mu^{(2)}_{exp.}$ would still be in agreement with the observed Stark-effect. I and II indicate CNDO/2-dipole moments calculated from the structures I and II of Table 7; α and β indicate dipole moments calculated by adding the experimental values for Thiophene and Benzonitrile vectorially (α with S at the negative end and β with S at the positive end in Thiophene). An unambiguous choice of μ_{exp} should be possible from the comparison of the Stark-effects in $H_{(4)}$ and $H_{(5)}$ deuterated 3-Cyanothiophene.

and with $\sphericalangle C_{(2)}C_{(3)}C_{(6)}$ changed from 123.3° to 121.2° reproduces all three observed rotational constants within 1 MHz. To appreciate this result better it may be noted that for a complete r_0-structure determination typical differences between observed and calculated rotational constants are on the order of 0.1 to 0.5 MHz. We therefore feel that the major changes of the ring structure due to $C_{(3)}$-Nitrile substitution indeed occur in the adjacent double bond.

As a routine measure we have also carried out CNDO/2-calculations [17] based upon the initial (column I of Table 7) and "improved" (column II of Table 7) structures. The results are listed in Table 6 (dipole moments) and at the bottom of Table 7 (total energies). In contradiction to the above result CNDO/2 total energies favour the initial "Thiophene-Benzonitrile-structure". (The total energy should reach a minimum for the equilibrium configuration.) On the other hand, the CNDO/2 dipole moments are in extremely poor agreement with the observed values. Such a poor agreement is frequently observed if CNDO/2 is applied to highly delocalized systems. In disregard of the CNDO/2 result for the total energies we are therefore confident that the "improved" structure listed in column II of Table 7 should lead to good predictions for the rotational frequencies of other species.

Table 7. Preliminary structures for 3-Cyanothiophene which were used in this work and the corresponding rigid rotor rotational constants and CNDO/2 total energies. I ring structure from Thiophene [22] and $-C\equiv N$ structure from Benzonitrile [23]. II structure from a fit of the $^rC_{(2)}C_{(3)}$ bond distance and the $\sphericalangle C_{(2)}C_{(3)}C_{(6)}$ bond angle to the observed rotational constants. Bond lengths and angles listed in the center column are the same for both structures.

Distances in Å units	I		II
$^rSC_{(2)} = {}^rSC_{(5)}$		1.714	
$^rC_{(2)}H_{(2)} = {}^rC_{(5)}H_{(5)} = {}^rC_{(4)}H_{(4)}$		1.08	
$^rC_{(4)}C_{(5)}$		1.370	
$^rC_{(3)}C_{(4)}$		1.423	
$^rC_{(3)}C_{(6)}$		1.451	
$^rC_{(6)}N$		1.158	
$^rC_{(2)}C_{(3)}$	1.370		1.346
Angles			
$\sphericalangle C_{(2)}SC_{(5)}$		92.17°	
$\sphericalangle SC_{(5)}C_{(4)}$		111.47°	
$\sphericalangle SC_{(5)}H_{(5)} = \sphericalangle SC_{(2)}H_{(2)}$		119.85°	
$\sphericalangle C_{(5)}C_{(4)}H_{(4)}$		123.28°	
$\sphericalangle C_{(3)}C_{(6)}N$		180.00°	
$\sphericalangle C_{(2)}C_{(3)}C_{(6)}$	123.28°		121.2°
Rotational constants	I	exp. values	II
A [MHz]	7.168 88	7.115 103	7.116 125
B [MHz]	1.473 649	1.491 292	1.492 964
C [MHz]	1.222 375	1.232 536	1.234 058
CNDO/2 total energies (atomic units)	−60.021 288		−60.021 082

Wir danken Herrn Prof. Dr. Dreizler für die Durchsicht des Manuskripts. Der Deutschen Forschungsgemeinschaft sei für die Bereitstellung von Personal- und Sachmitteln gedankt. Die Rechnungen wurden auf der PDP 10-Anlage des Rechenzentrums der Universität Kiel durchgeführt.

[1] J. Wiese, L. Engelbrecht, and H. Dreizler, Z. Naturforsch. **32a**, 152 [1977].
[2] L. Engelbrecht and D. H. Sutter, Z. Naturforsch. **31a**, 670 [1976].
[3] D. H. Sutter and W. H. Flygare, Topics in Current Chemistry **63**, 89 [1976].
[4] S. Nishimura and E. Imoto, Nippon Kagaku Zasshi **82**, 1411 [1961].

[5] H. D. Rudolph, Z. Angew. Phys. **13,** 401 [1961].
[6] U. Andresen and H. Dreizler, Z. Angew. Phys. **30,** 207 [1970].
[7] D. Sutter, Z. Naturforsch. **26 a,** 1644 [1971], Fig. 7.
[8] F. Mönnig, Dipl. Thesis, Freiburg 1963, p. 50–55.
[9] H. J. Tobler, H. U. Wengler, A. Bauder, and H. H. Günthard, J. Sci. Instr. **42,** 240 [1965].
[10] J. K. G. Watson, J. Chem. Phys. **46,** 1935 [1967].
[11] V. Typke, Z. Naturforsch. **26 a,** 1775 [1971].
[12] J. K. G. Watson, J. Chem. Phys. **46,** 1935 [1967], Equation (67).
[13] H. D. Rudolph, Z. Naturforsch. **23 a,** 540 [1968].
[14] S. Golden and E. B. Wilson jr., J. Chem. Phys. **16,** 669 [1948].
[15] D. R. Lide jr., J. Chem. Phys. **22,** 1577 [1954].
[16] T. Ogata and K. Kozima, J. Mol. Spectr. **42,** 38 [1972].
[17] J. A. Pople and D. L. Beveridge, Approximate Molecular Orbital Theory, McGraw-Hill Book Comp., New York 1970.
[18] C. H. Townes and A. L. Schawlow, Microwave Spectroscopy, McGraw-Hill Book Company, New York 1955, Chapter 6.
[19] J. S. Muenter, J. Chem. Phys. **48,** 4544 [1968].
[20] L. Pauling, Die Natur der chemischen Bindung, Verlag Chemie GmbH, Weinheim (Bergstraße) 1968, p. 227.
[21] See listing of fundamental constants in Ref. [18].
[22] J. Casado, L. Nygaard, and G. O. Sorensen, J. Mol. Struct. **8,** 211 [1971].
[23] B. Bak, D. Christensen, L. Hansen-Nygaard, and J. Rastrup-Andersen, J. Mol. Spectr. **7,** 58 [1961].